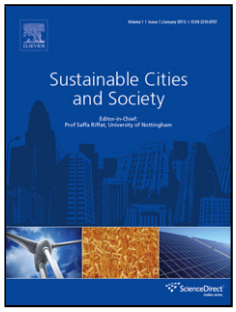

Title: Comparative and combinative cooling effects of different spatial arrangements of buildings and trees on microclimate

Authors: Zhifeng Wu, Panfeng Dou, Liding Chen

PII: S2210-6707(18)32698-2
DOI: https://doi.org/10.1016/j.scs.2019.101711
Article Number: 101711

Reference: SCS 101711

To appear in:

Received date: 25 December 2018
Revised date: 11 July 2019
Accepted date: 11 July 2019

Please cite this article as: Wu Z, Dou P, Chen L, Comparative and combinative cooling effects of different spatial arrangements of buildings and trees on microclimate, *Sustainable Cities and Society* (2019), https://doi.org/10.1016/j.scs.2019.101711

Comparative and combinative cooling effects of different spatial arrangements of buildings and trees on microclimate

Zhifeng Wu[a], Panfeng Dou [a,b], Liding Chen[b,c*]

Full affiliations: [a] Key Laboratory of Urban Environment and Health, Institute of Urban Environment, Chinese Academy of Sciences, Xiamen 361021, China

[b] University of Chinese Academy of Sciences, Beijing 100049, China

[c] State Key Laboratory of Urban and Regional Ecology, Research Center for Eco-Environmental Sciences, Chinese Academy of Sciences, Beijing 100085, China

E-mail address of authors: iamwuzf@163.com (Zhifeng Wu); pfdou@iue.ac.cn (Panfeng Dou); liding@rcees.ac.cn (Liding Chen)

Highlights:

- Three contributory factors were considered to evaluate variations in thermal microclimates.
- The cooling effectiveness of greenspace is non-linear relative to area.
- Intense solar irradiation suppresses the cooling effect of high vegetation cover.

Abstract

The amounts and arrangements of buildings and trees are primarily responsible for controlling small-scale thermal environments. However, uncertainties exist about how such structures regulate microclimates in cities. We investigated the effects of three contributory factors on microclimates: building arrangement, amount of land covered by tree canopies, and the intensity of solar irradiation relative to latitude. We modeled microclimate with the high spatial and temporal resolution ENVI-

met model and validated it with *in situ* measurements. We designed and modeled seventy-two idealized model scenarios to compare cooling effects of various combinations of the contributory factors to microclimate. We found that: (1) both building and tree arrangements influence thermal microclimates (i.e., high-rise developments provide more land for greenspace and lead to lower near-surface temperatures than low-rise developments), (2) more area of forested greenspace leads to a more significant cooling effects (but the cooling effect of forested greenspace is non-linear relative to area), and (3) intense solar irradiation suppresses the cooling effects of greenspaces. Our results underscore the practical implications of shading arrangements on the evolution of thermal environments in high-density cities, which is useful for planning and designing mitigation strategies in urban areas and developing action plans at the neighborhood scale.

Key words: urban heat island, mitigation, ENVI-met, urban planning

1. Introduction

Urbanization is one of the most significant drivers of global change (Tian, & Qiao, 2014). Material cycling and energy balance are dramatically altered during urbanization (Shi, & Yang, 2014), which can lead to a variety of environmental problems and directly threaten the wellbeing of urban residents. The urban heat island (UHI) effect is one of the most obvious ramifications of urbanization. This effect is caused by man-made alterations to urban surfaces (such as replacing vegetation with heat absorbing structures), which resulted in increasing the release of waste heat (Oke, 1987). High temperatures sometimes cause severe health problems, including respiratory problems, cardiovascular and cerebrovascular diseases, and even death, especially for senior citizens (Li, Zhou, Cai, Zhang, & Pan, 2011; Wong, Alias, Aghamohammadi, Aghazadeh, & Nik Sulaiman, 2017). A strong association has been reported between higher temperatures and increased mortality (Ward, Lauf, Kleinschmit, & Endlicher, 2016; Zeng et al., 2014). Therefore, it is imperative to develop effective strategies to mitigate UHI effects, especially for cities with high population densities. Areas of higher population density are likely to have a higher amount of development and impervious surfaces, and potentially experience more severe urban heat island effects due to the thermal properties of the built-up environments (Hondula & Barnett, 2014).

The urban landscape is a highly complex and heterogeneous system, consisting of a diversity of man-made objects and natural features, such as trees. The three-dimensional urban morphology obviously impacts the spatial-temporal variability of solar heat gain on urban surfaces, which is a major contributing factor to changes in urban climate (Yu, Liu, Wu & Lin, 2009; Wang et al., 2017). Buildings and trees are the two principal components of three-dimensional urban landscapes leading to the redistribution of solar radiation, which is the primary heat input in urban areas. Optimizing

the relative amount and arrangement of these two components has proven to be effective in regulating microclimatic conditions in urban environments (Ghaffarianhoseini, Berardi, & Ghaffarianhoseini, 2015; Liu, Theller, Pijanowski, & Engel, 2016; Ratti, Raydan, & Steemers, 2003; Taleb, & Abu-Hijleh, 2013).

The configuration of buildings is important in influencing wind flow patterns in street canyons (Xie, Huang, & Wang, 2005), which significantly impacts the release of sensible heat, the dispersion of air pollutants, and thermal comfort. In addition, buildings can control microclimate by modifying solar radiation on street surfaces, which in turn impacts ground surface temperatures and near-surface air temperatures. It has been suggested that optimizing building arrangements are more effective in controlling heat exchange than modifying thermal characteristics, such as modifying thermal conductivity, heat capacity, or the albedo of building materials (Andreou, 2014). Vegetation achieves its cooling effect mainly via evaporative cooling and passive shading (Tan, Wong, Tan, Jusuf, & Chiam, 2015). Although a single tree can moderate its surrounding microclimate, an aggregation of trees, such as an urban forest, can extend its temperature moderating effects to a greater distance (Vaz Monteiro, Doick, Handley, & Peace, 2016). The extent of cooling effects by forested greenspace is influenced by the size, spatial pattern, and composition of trees, the layout (arrangement) of surrounding urban structures, and prevailing wind patterns (Xiao, Dong, Yan, Yang, & Xiong, 2018; Yu, & Hien, 2006). Numerical models have been employed to explore the cooling capacities of buildings and greenspaces at various spatial scales from the neighborhood to the city scale (Chang, & Li, 2014; Chow, Pope, Martin, & Brazel, 2011; Coseo, & Larsen, 2014; Sodoudi, Zhang, Chi, Müller, & Li, 2018; Xu et al., 2017; Yin, Yuan, Lu, Huang, & Liu, 2018). Although the density and arrangement of buildings and the coverage and types of vegetation have been shown to

be the most critical factors impacting local thermal environments, few studies have compared the effects of various combinations of building arrangements and tree coverages on thermal conditions.

Stewart (2011) categorized urban landscapes into 17 different local climate zones (LCZs), each characterized by structural and land cover properties that influence air temperature at the street level. These LCZs have been employed by many researchers to represent the heterogeneity of urban thermal environments (Leconte, Bouyer, Claverie, & Petrissans, 2015; Lehnert, Geletič, Husák, & Vysoudil, 2014, 2015; Unger, Skarbit, & Gál, 2018; Wang, & Ouyang, 2017). In fact, LCZs are likely to become more widely used in modelling urban climates because they capture most of the essential morphological characteristics that influence urban temperature regimes (Verdonck et al., 2018; Giridharan, & Emmanuel, 2018). LCZs can be further subcategorized into two subtypes: built types and landcover types. The LCZs for built types typically use artificial landscape attributes to differentiate features (e.g., percent of viewable sky, percent building surface, percent impervious surface, and percent pervious surface). Although buildings and vegetation co-exist in most urban settings and both are responsible for shaping local thermal environments, vegetation coverage has received less attention and it seems to introduce more uncertainty in the evaluation of local environments. We believe that it would be useful to evaluate various combinations of building arrangements and vegetation coverages relative to their impacts on thermal environments. Therefore, in this study we address the following questions:

1. What are the main driving forces shaping a local thermal microclimate under specific weather conditions?

2. How much mitigative effect can be achieved by changing building arrangements and/or urban forest cover?

In this study, we applied numerical model to investigate effects of various building configurations and vegetation coverages (and combined effects of both landscapes types) on thermal conditions at street level. Also, we took into account the sun's angle of incidence to investigate the potential ways to mitigate UHI effects in cities located at various latitudes. We used the high spatial and temporal resolution microclimate model ENVI-met and then validated the model with *in situ* measurements in a typical, multi-story, urban residential development (at both high-rise and low-rise apartment buildings). We tested 72 scenarios in all aiming to explore the comparative and combinative effects of above-mentioned three factors on micro-environments.

2. Methods

2.1 Study area

Beijing (Fig. 1a), the capital of China, covers 16,808 km^2 and has a continental climate characterized by hot and wet summers and cold and dry winters. Beijing has experienced rapid urbanization in past 30 years along with a substantial increase in the use of motorized vehicles. Since 1978, when the reform and opening-up policy was initiated, Beijing has drawn a large number of people from other (primarily rural) regions of the country. By 2016, there were 21.7 million people living in Beijing, with a highest concentration of people living near city's center.

The real estate market in Beijing has experienced a massive housing-construction boom ever since the welfare housing distribution policy was abolished in the mid-1990s (Le, & Jinsheng, 2008). However, the steadily increasing numbers of immigrants have outstripped the supply of housing, especially in Beijing's urban center. To reduce the population pressure in the central districts of Beijing, several large residential urban developments have been constructed in outlying suburban

areas [e.g., the Tiantongyuan-Beiyuan residential area (TBRA)] to accommodate the growing numbers of immigrants to the city (Fig. 1b). The population density in the TBRA is now even higher than in the two central urban districts of Beijing. There are few neighborhood parks in the TBRA and those few are unevenly distributed. However, the few greenspaces that exist in residential sections of the city provide many environmental and social benefits to residents.

We selected the Tianrunfuxi Residential Quarter (TRQ) located in the TBRA district (Fig. 1c) to measure thermal microclimate conditions associated with various combinations of building configurations and forested greenspaces. The TRQ consists of 18 apartment buildings (eight 21-story buildings and ten 5-story buildings) accommodating approximately 3500 households. The TRQ covers 10.3 ha, representing a typical population density for residential developments in and around Beijing (Fig. 1).

Besides Beijing, we also chose two other cites (Changchun and Xiamen) at different latitudes to investigate the effects of the intensity of solar irradiation relative to latitude on microclimate. Same building arrangement and tree coverage scenarios of Beijing were applied to these two cities.

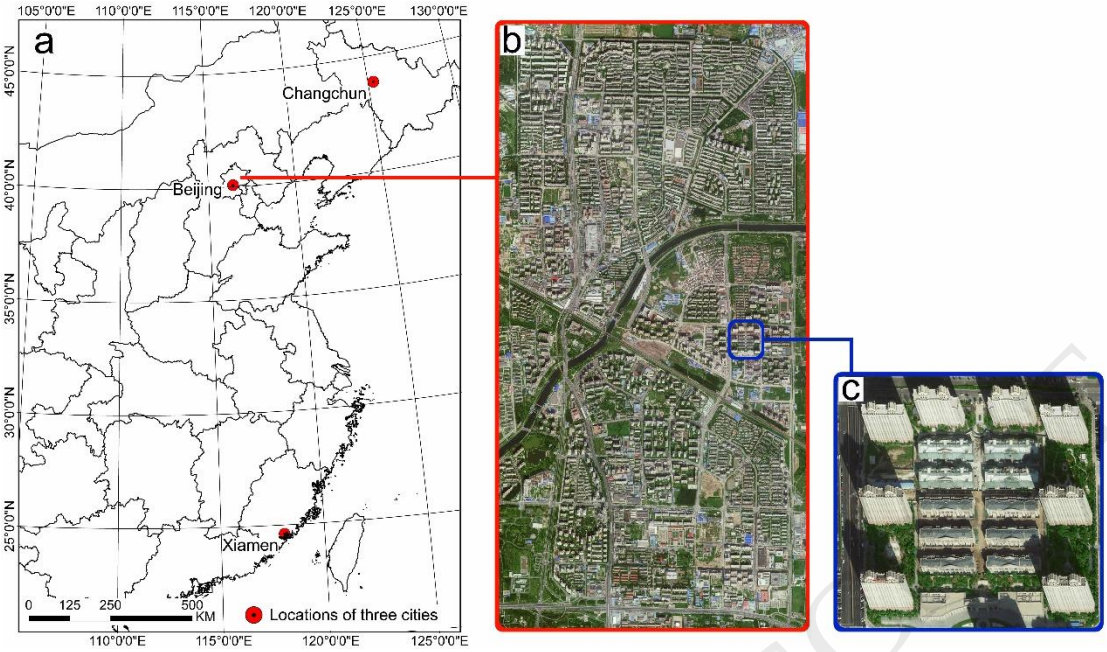

Fig. 1 BaiduMap® image of the study area. a: location of the three study sites: Changchun (43.88° N, 125.35° E), Beijing (39.54° N, 116.24° E), and Xiamen (24.49° N, 118.13° E); b: aerial view of the Tiantongyuan-Beiyuan Residential Area (TBRA); c: aerial view of the Tianrunfuxi Residential Quarter (TRQ) . (BaiduMap® is a desktop and web mapping service provided by Baidu Inc., offering high-resolution satellite imagery).

2.2 Numerical model

The ENVI-met model was selected to model variations in the thermal environmental of urban housing complexes. The typical spatial resolution of the model is ~0.5-10 m, which makes the resolution suitable for simulating interactions between micro-scale factors that shape the environment. ENVI-met is a three-dimensional and non-hydrostatic, prognostic numerical model with computational fluid dynamics (CFD) as its core algorithm. The model considers detailed heat transfers processes related to a variety of parameters, including:

1. Absorption of shortwave and longwave radiation and reflection of building exteriors and

plant surfaces; and,

2. Evaporation, transpiration, and sensible heat flux to the atmosphere from vegetation.

The ENVI-met model has been widely used and validated for assessing built environments (Berkovic, Yezioro, & Bitan, 2012; Carfan, Galvani, & Nery, 2012; Johansson, Onomura, Lindberg, & Seaquist, 2015; Skelhorn, Lindley, & Levermore, 2014; Taleghani, Tenpierik, van den Dobbelsteen, & de Dear, 2013). ENVI-met requires two user-defined input files. One is the area input file, a 3-dimensional representation that allows the user to depict the layout of buildings, vegetation, artificial surfaces, and soils. The other input file is a configuration file that contains meteorological parameters and surface properties for initializing the model and computing energy exchange. We used high-resolution BaiduMap® images and field measurements to delineate the configuration of buildings and greenspaces of TRQ as accurately as possible. A main area of the model domain, representing current conditions, was built with $117 \times 109 \times 20$ three-dimensional cells, wherein each cell had dimensions $3 \times 3 \times 7.5$ m. Although the area represented by the core model was defined with the area input file, additional grids can be added around the perimeter of the main area to shift the model boundary away from the area of interest and to minimize potentially complicating boundary effects. That is, a buffer zone can be created outside the core area to solve problems with the model not working reliably at and near the borders of the core area. In the present study, we added a 10-grid-deep border to the perimeter of the model to enhance stability when simulating elements located close to the border of the main model domain.

To investigate the effects of building arrangements on microclimate, two scenarios were developed: (1) a high-rise scenario that replaced all currently existing low-rise apartment buildings with high-rise buildings (Fig. 2a) and (2) a low-rise scenario that replaced all existing high-rise

apartment buildings with low-rise buildings (Fig. 2b). The separation distance between adjacent buildings was decided by sunlight analysis to ensure adequate sunlight exposure for each floor throughout the year ($d = \frac{h-h1}{\tan\theta}$) (Fig. 2c). Therefore, in the high-rise model scenario, we utilized 12 apartment buildings (including four buildings we added to the array). Due to the lower height of buildings in the low-rise model scenario, we added 18 buildings to the 8 already present. The newly added buildings were located on land previously occupied by high-rise apartment buildings. According to the allowed separation distance between adjacent buildings in Beijing, 18 apartment buildings, at most, can be added under a low-rise model scenario.

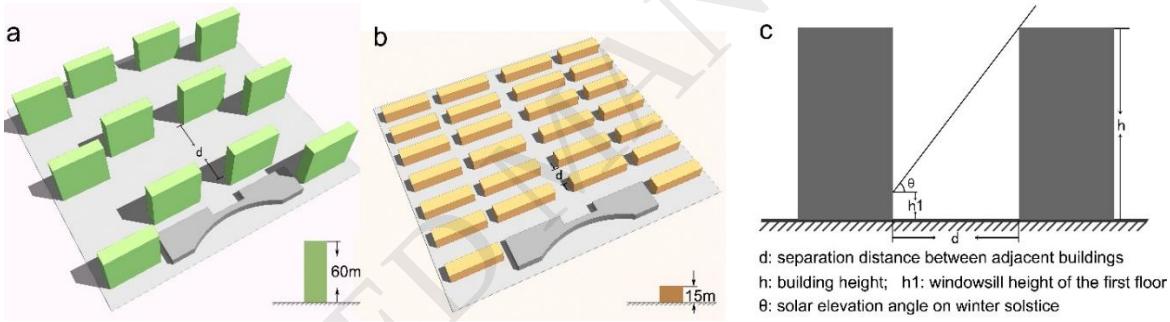

Fig. 2 Building arrangement scenarios. a: High-rise scenario; b: Low-rise scenario; c: Parameters for calculating the separation distance between adjacent buildings

Based on the current TRQ's landscape, the land use can be categorized into three types: buildings, roads and greenspace. The layout of buildings and/or roads is usually designed first when planning a new residential area and then greenspace is planned for land patches between buildings and roads. Although the building/unit area of high-rise buildings is 14.1% lower than low-rise buildings, the volume of buildings is 1.64 times higher under the high-rise scenario, meaning that

the high-rises can house more people per unit area. In addition, land area used for roads is 1.38 times less under the high-rise scenario than under the low-rise scenario because there are fewer buildings to access. To simplify the model, we assumed that land not used for buildings and roads could be used for greenspace. Under this assumption, we could estimate the cooling effects of two building arrangement scenarios with the same percentage of greenspace, and further analyze the impact of building arrangement on local thermal environment. Because the footprint of buildings under the high-rise scenario was less than under the low-rise scenario and the road footprint was also lower, the high-rise scenario provided 18.7% more land available for greenspace than the low-rise scenario (Table 1).

Table 1 Basic information of landscape composition of two building arrangement scenarios modeled in this study

Scenarios	Area (ha) of TRQ	Footprint of buildings/area TRQ (%)	Footprint of roads/area TRQ (%)	Footprint of greenspace/area TRQ (%)	Building volume (m^3)
High-rise	10.3	14.9	11.9	73.2	699,945
Low-rise	10.3	29.0	16.5	54.5	427,173

Based on the two building configurations we adopted, we examined 12 different forest coverages as greenspace (0%, 5%, 10%, 15%, 20%, 25%, 30%, 35%, 40%, 45%, 50%, and 55%) to investigate various combinations of building footprints and greenspace for each building arrangement we modeled. According to the code dealing with planning and designing urban

residential areas (Chinese Code GB-50180-93), there should be no less than 30% greenspace in any new residential development.

In addition to testing our model for conditions in Beijing, we also tested the model (with the same building configurations and forested greenspace coverages) for two other cities in China: Changchun and Xiamen (subtropical) (Fig. 1a). These three cities, located at different latitudes, were chosen to analyze the impact of irradiation angle on near-surface microclimates. In total, we tested 72 combinations: 2 building configurations × 12 forested greenspace coverages × 3 latitudes.

2.3 Statistical analyses

Statistical analyses were performed with SPSS software (Version 19). Paired sample *t*-tests were performed to address whether the cooling effects of various tree canopy coverages under the two tested building configurations differed at specific points in time. We calculated the root mean squared error (RMSE), mean average error (MAE), mean bias error (MBE), and the index of agreement to evaluate the accuracy of our simulation results. RMSE is the square root of the average of squared differences between prediction and actual observation; MAE measures the average magnitude of the errors in a set of predictions, without considering their direction; MBE describes the direction of the error bias. Its value is related to magnitude of values under investigation; The index of agreement (d) is a standardized measure of the degree of model prediction error and varies between 0 and 1. A value of 1 indicates a perfect match, and 0 indicates no agreement at all. These four indices are commonly used to measure accuracy for continuous variables. They are calculated with equation (1) to (4):

$$\mathrm{RMSE} = \sqrt{\frac{1}{n}\sum_{i=1}^{n}(P_i - O_i)^2} \quad (1)$$

$$\mathrm{MAE} = \frac{1}{n}\sum_{i=1}^{n}|P_i - O_i| \quad (2)$$

$$\mathrm{MBE} = \frac{1}{n}\sum_{i=1}^{n}\frac{P_i - O_i}{O_i} \quad (3)$$

$$\mathrm{d} = 1.0 - \frac{\sum_{i=1}^{n}|O_i - P_i|}{\sum_{i=1}^{n}(|P_i - \hat{O}| + |O_i - \hat{O}|)} \quad (4)$$

Where P_i is the predicted values of air temperature; O_i is the measured values of air temperature; $\hat{O}$ is the average of measured values; n is the number of measurements of air temperature, which is 31 in present study.

3. Results

3.1 Model validation

We compared the ENVI-met model outputs with meteorological data collected from 10-18 August 2014 at a nearby residential quarter (~1.0 km away from TRQ). Six HOBO® pro v2 loggers were mounted on tree trunks or electrical poles at the height of 2 m to prevent sabotage of data loggers. We chose 14 August 2014 to model the thermal performance of the various building and vegetation arrangement scenarios. The modeled temperatures represent mean air temperature at 2 m above ground throughout the entire modeled area, whereas we obtained the measured air temperatures from data loggers located at residential apartments. Both measured and predicted air temperatures peaked at 14:00, but showed different rates of change throughout the course of the day (Fig. 3). Measured temperatures increased 1.11 ℃ per hour during the 7:00-14:00 period and decreased 0.67 ℃ per hour after 14:00. According to results, RMSE was 1.05 °C, MAE was 0.95 °C, and MBE was -0.49 °C. The index of agreement was 0.95, which indicates that even though measured temperatures were generally higher than predicted temperatures throughout most of the

day (at 2 m above ground), the model generally showed good agreement with field measurements.

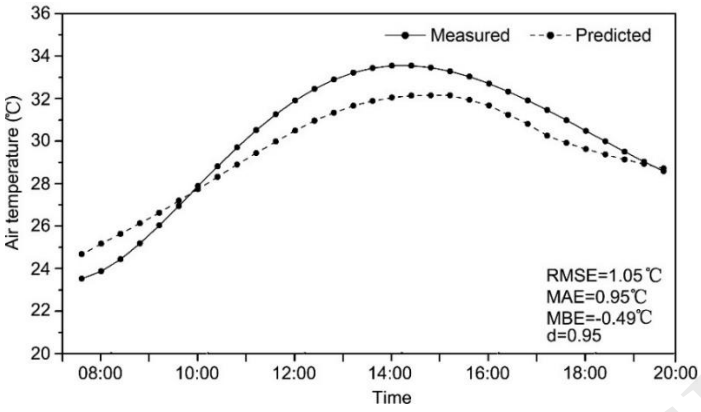

Fig. 3 Mean hourly averaged air temperature measured by meteorological stations (solid curve) and predicted by the ENVI-met model (dotted curve). Temperatures from the ENVI-met simulations were for at 2.0 m above ground. RMSE = root mean squared error; MAE = mean absolute error; MBE = mean bias error; d = index of agreement

3.2 Variation in near surface air temperature under various building arrangement scenarios

Air temperature near the land surface is one of the key parameters associated with thermal comfort experienced by humans in cities. We extracted averaged air temperature at three different times during the day: morning (8:00), midday (14:00), and night (20:00). We modeled near-surface temperatures (2.0 m above ground) to determine how heat at street level might be altered by adding more forest to surrounding non-impervious areas. For both high-rise and low-rise building arrangements, mean air temperatures declined as percent cover of forested greenspace increased. Specifically, the air temperatures (at 2.0 m) were cooler under the high-rise scenario than under the low-rise scenario for all greenspace coverages at all three times of day examined. Although statistically significant differences were identified for these mean air temperatures, the temperature

differentials at 8:00 and 20:00 showed different trends in variations in contrast with 14:00. The temperature differential between the two building arrangement scenarios was higher with higher forest coverage for 8:00 and 20:00 (Fig. 4). At 8:00 without greenspace, the differential in mean air temperature was negligible (<0.1℃ difference) between the high- and low-rise scenarios. However, the temperature differential widened with incrementally higher forest coverage (more forested greenspace), with a peak differential in temperatures (0.2 ℃) occurring at the highest forest cover modeled (55%) (Fig. 4a). In addition, the variation in air temperatures (calculated as one standard deviation) increased perceptibly under both building arrangement scenarios as forest cover increased from 0% to 55%. By 20:00 (night), the variation between the two building arrangements and the downward trend in air temperatures with higher forest coverages were similar to the trends exhibited at 8:00, except that the differential in mean air temperatures were much wider (0.11 ℃ at 0% canopy cover and 0.73 ℃ at 55% cover) (Fig. 4c). However, at 14:00 the temperature differential and the variation in air temperatures remained basically unchanged for 0% to 55% forested coverages (Fig. 4b).

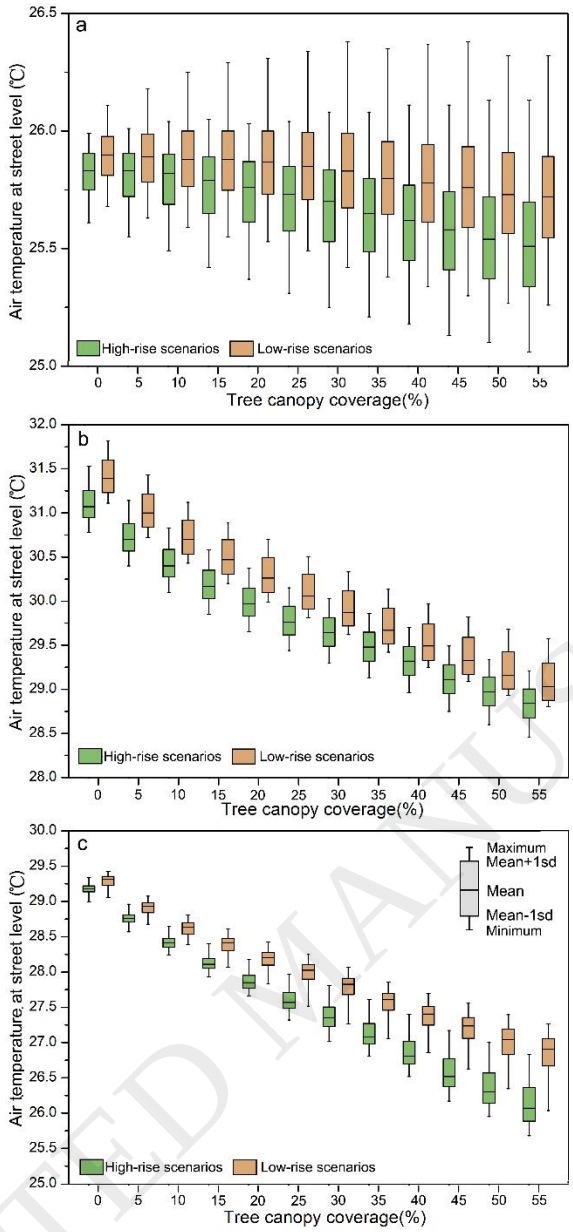

Fig. 4 Variations in air temperatures under two building configurations and 12 tree coverages at three times in Beijing. a: 8:00 (morning); b: 14:00 (midday); c: 20:00 (night).

The relationship was curvilinear between temperature reductions at street level and higher forested coverage. That is, the rate of reduction in temperatures tended to decline from one 5% canopy cover increment to the next higher canopy cover (as amount of shading and/or evapotranspiration cooling increased). In both the high- and low-rise scenarios, the highest

incremental reduction in temperature was the greatest from the 0% forest cover to the 5% forest cover. For example, at 14:00 in the high-rise scenario, street-level temperature declined by 0.38 ℃ from 0% to 5% canopy cover and 0.30 ℃ from 5% canopy cover to 10% cover. Likewise, at night (20:00), the rate in temperature reduction declined gradually as the amount of tree canopy increased (even though absolute temperatures were lower at higher canopy covers). The difference is that there was statistically significant difference in temperature reduction related to amount of forest coverage between the two building configurations at 20:00. Furthermore, each increasing 5% increment in forest cover under the high-rise scenario resulted in higher cooling capacity at 20:00 (Fig. 5a, 5b).

We applied exponential regression models to compare the mean reduction in air temperature at street level against increases in forest coverage. The regression models for both high-rise and low-rise scenarios at midday and high-rise scenarios at night showed high fitting accuracies (R^2 = 0.887, 0.935, and 0.813, respectively). At two times (14:00 and 20:00), the cooling power (measured as air temperature) of the increased tree canopy coverage was rapidly less influential at incrementally higher coverages (Fig. 5a', b'). The first 5% increment (0→5%) in forest cover showed approximately 3 times higher cooling power comparing with the last 5% increment (50%→55%) of tree canopy coverage for both high-rise and low-rise scenario at midday. Although the difference between the first and the last 5% increment in forest cover at 20:00 reduced slightly, the first 5% increment still showed more powerful cooling capability in contrast with the last 5% increment on the basis of 50% tree canopy coverage for the two building configuration scenarios.

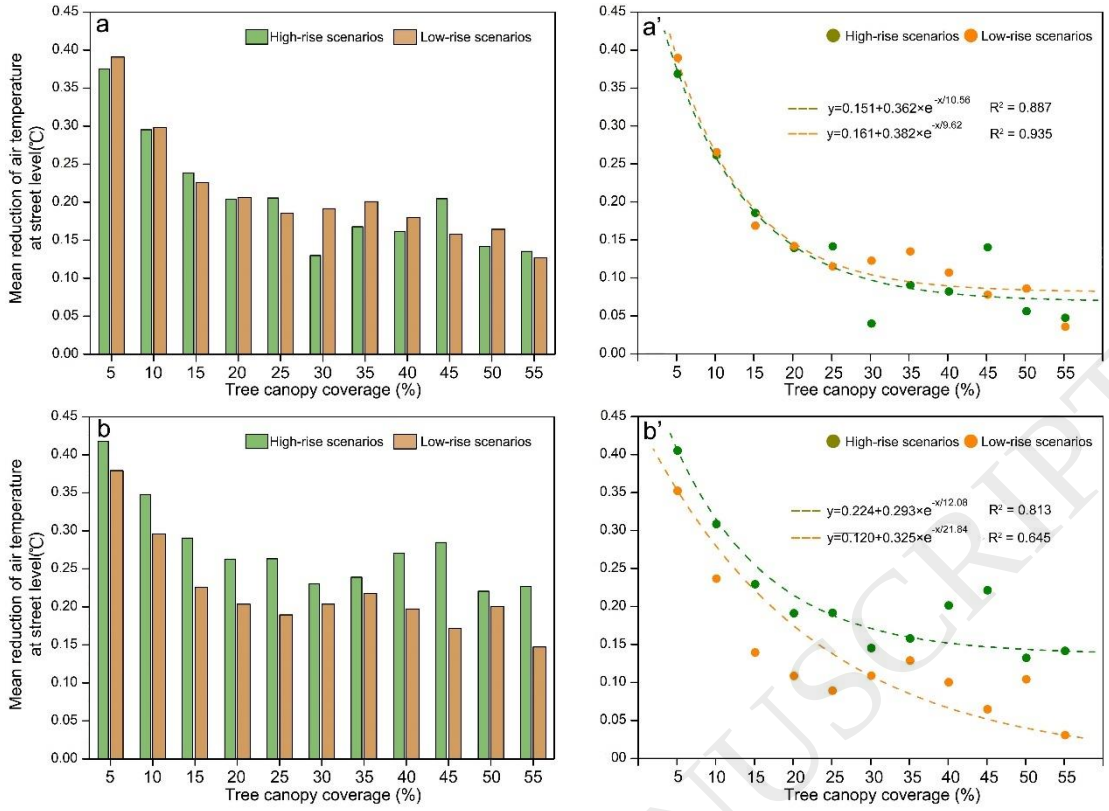

Fig. 5 Mean reduction in air temperature for each 5% incremental increase in tree canopy cover at midday and night. (a) 14:00 (midday), (b) 20:00 (night). Exponential regression results calculated for midday (a': 14:00) and night (b': 20:00)

3.3 Variation of near surface air temperature related to latitude

Because solar radiation is the driving force behind surface thermal fluxes [i.e., surface temperatures primarily depend on incident solar irradiation levels (Yang, & Li, 2015)], we modeled heat impacts in two other cities, one city located at a much lower latitude than Beijing (Xiamen) and the other at a higher latitude (Changchun) (Fig. 1a). For Xiamen, there were much higher air temperatures at midday for both the high- and low-rise building arrangements than in Beijing and Changchun. However, by 20:00 (night), the temperature differential between Xiamen and two other cities were much less. In the low-rise scenarios, the near-surface air temperatures of Beijing were

closer to temperatures of Xiamen than Changchun, although the latitude differential between Beijing and Changchun is less than between Beijing and Xiamen (Fig. 6).

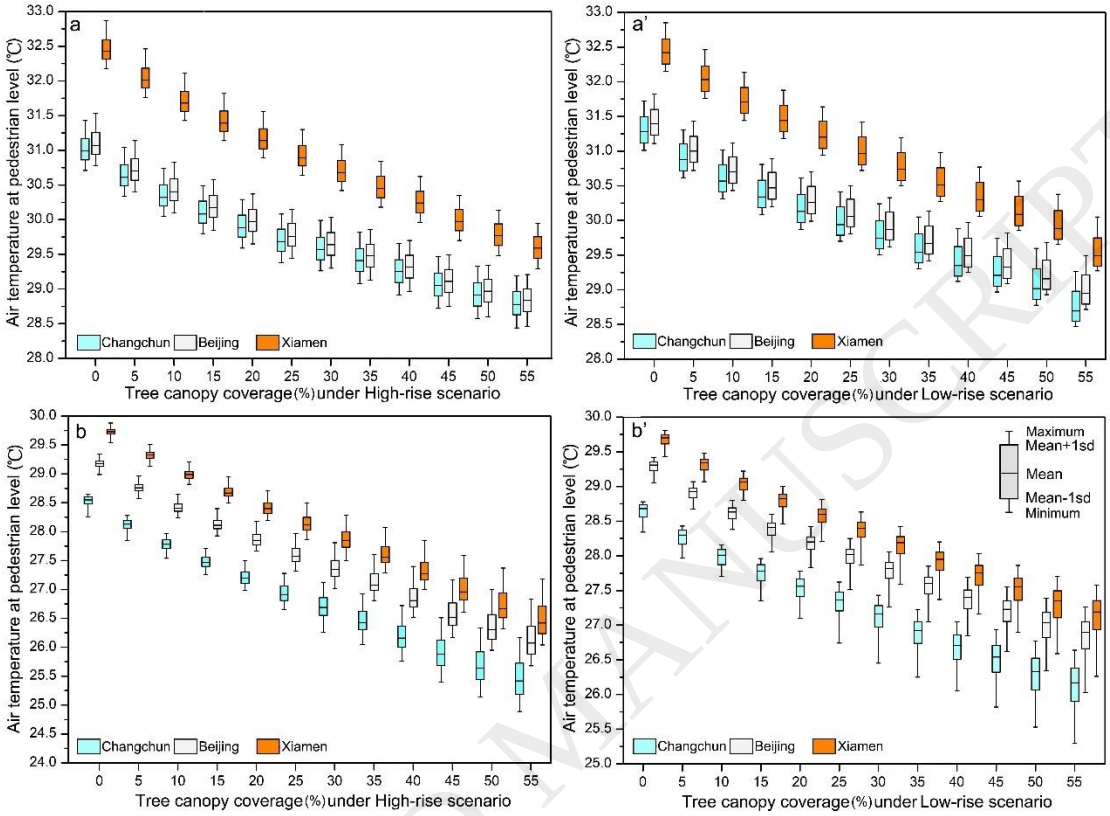

Fig. 6 Variation of air temperatures of different building arrangement and vegetation coverage scenarios at three cities. a: 14:00 (midday) of high-rise scenario; a': 14:00 (midday) of low-rise scenario; b: 20:00 (night) of high-rise scenario; b': 20:00 (night) of low-rise scenario.

4. Discussion

4.1 The effect of building arrangement and vegetation coverage on air cooling

Increasing vegetation coverage in urban areas has long been proposed as a potentially viable strategy for helping combat the UHI effect (Bowler, Buyung-Ali, Knight, & Pullin, 2010). It is

important to select tree species appropriate for urban environments (ones that can tolerate pollution and other urban stresses) and optimize their spatial arrangements. In addition, it is equally important to determine if there is an optimal canopy coverage that can both help create a more comfortable thermal environment in cities and be compatible with the high intensity of infrastructure existing in urban environments.

A number of empirical and simulation studies have investigated the impact of greenspace on ambient air temperatures at a variety of spatial scales (Li, Zhou, Ouyang, Xu, & Zheng, 2012; Middel, Chhetri, & Quay, 2014; Skelhorn, Lindley, & Levermore, 2014). At the neighborhood scale, Middel et al. (2014) showed that there is a negative linear relationship between the amount of tree canopy and air temperature (i.e., a 0.14 ℃ reduction in air temperature per 1% increase in tree canopy cover). In our study, we also found that tree canopy coverage is negatively associated with air temperature near street level. However, in Beijing the relationship we found for both high- and low-rise building was not linear. In addition, the absolute reduction in temperature of 1% tree canopy cover increase on coverage was significantly lower than what Middel et al. (2014) modeled for a city located in a hot desert climate. The major differences between our study and Middel's study are that the two studies were conducted in different climates (temperate vs. desert) and there were different parameterizations and assumptions used in the two microclimate models. Besides, the two studies differed in the cooling potential for the same coverage of tree canopy. In our study, the first 5% increment of tree canopy coverage leads to obviously more cooling than provided by any additional increases in canopy cover. The decline in cooling capacity provided by incrementally increasing canopy (from ~0.4 ℃ to less than 0.15 ℃) could be explained by a variation in shading effects and transpiration rates of tree species. Larger greenspace areas tend to have stronger cooling

and humidification effects. However, for every single tree in a forest, its cooling capability would decrease with increased area of tree patch size. That is, when trees are sparsely distributed, every single tree can reach its full potential for lowering air temperature (by intercepting incoming solar radiation and evapotranspiration process). Thus, a dense forest with overlapping leaves reduces the contribution of an individual tree's ability to cool the surrounding atmosphere by limiting its ability of block incoming solar irradiation. Moreover, Jiao et al. (2017) demonstrated that the transpiration rate of trees (cooling effectiveness) declines as tree patch size increases. So, as canopy coverage increases, the cooling capacity gradually declines.

Our results showed that there was a non-linear relationship between tree canopy cover and cooling effect. Considering that the amount of land that can be used for tree canopy in rather limited in cities, we would expect that an optimal tree canopy cover might exist for a specific building arrangement scenario under certain climatic condition. This optimal mix of building arrangement and vegetation coverage would be the most comfortable thermal environment for people living in densely populated urban areas. In future studies, more field monitoring and numerical modelling should be conducted on the basis of building arrangement. A morphological classification system could be developed to identify optimal thresholds of vegetation coverage that maximize cooling efficiency in cities based on building configurations.

4.2 The effect of solar elevation on air cooling

Solar radiation is the primary source for heat gain in urban landscapes. The intensity of solar radiation is directly related to the sun's angle of incidence. Changing building layouts and increasing the amount of forested greenspace would be effective in influencing microclimatic conditions nearby. Analyzing the complex interactions between building arrangements and forest cover would

enhance our understanding of the mechanisms that impact the thermal variations exhibited by urban environments. Comparing the modeled near surface air temperature between high- and low-rise building arrangements at two times and three cities, only the high- and low-rise scenarios at 14:00 (midday) of Xiamen city showed no significant difference, which suggested that higher solar elevation can narrow the temperature difference, and strong solar irradiation might cause a temporary failure of mitigation strategies. Although there were statistically significant differences between two building arrangements scenarios at both 14:00 and 20:00 for Beijing and Changchun, the cooling effects of each increment of forested coverage differed between these two times of day (midday and night). At 20:00, with incrementally higher greenspace coverage, the high-rise scenario showed an obvious gradually increase in cooling capacity. At 14:00, the temperature differentials between two building arrangement scenarios were remained unchanged for all greenspace coverages from 0% to 55%. This indicates that strong solar radiation at midday could suppress the cooling effects of mitigation strategies, such as increasing greenspace to less than 55%.

Although our data on the influence of solar irradiation on microclimate can contribute useful information for planning future residential developments, there are still some practical limitations to the predictive ability of our models, particularly for cities located at various latitudes. First, for model simplicity and for making comparisons between cities easier, our models assumed identical building arrangements for all three cities. However, spacing of multistory buildings (specified by Chinese Code GB-50180-93 for planning and designing residential areas) is based on the sun's altitude at winter solstice, which varies with latitude. Therefore, buildings in residential sectors of more southern latitudes (e.g., Xiamen in the subtropics) can be more closely spaced (with less intervening spaces) than buildings in more northerly latitudes (e.g., Beijing and Changchun).

Second, for modeling purposes, we assumed that greenspace consisted of one and the same tree species (*Acer mono* Maxim.) for all model scenarios. However, cities differ in the composition of trees in their greenspaces (based on local climatic conditions and preferences). Therefore, the predictive power of the model could be improved by applying the spacing of multistory buildings and using the relative abundances of tree species actually occurring in modeled cities.

4.3 Implications on improving urban thermal environment

According to an observational and numerical modeling by Stewart (2011), during calm atmospheric conditions, temperature contrasts between various LCZ classes with significantly different building geometries (physical layouts) and landcover types can exceed 5 ℃, whereas more similar LCZ classes might vary by less than 2 ℃. Stewart (2011) concluded that those temperature contrasts were influenced largely by impacts of building layouts and land cover types. However, data from our study suggests that the differences in cooling effects related to building arrangement might not be apparent (or be masked) due to the intense solar irradiation that occurs in the middle of the day. Recently, researchers have increasingly applied the LCZ classification system to urban environments to help forecast conditions associated with thermal stress in urban environments by monitoring daytime temperatures or by interpreting thermal infrared remote sensing imagery. Our data suggests that forecasters should focus more on variations in thermal conditions that occur after sunset when the impacts of buildings and greenspace on the thermal environment are more discernable.

An increase in population densities of urban areas, especially megacities (e.g., Beijing), will be accompanied by massive construction activities and rapid urbanization. High-rise buildings are generally considered more resource efficient (per capita) than low-rise buildings because they

reduce transportation-related impacts (and thus air pollution and CO_2 emissions), are more efficient at recycling water and sewage, relieve development pressure on arable lands (except where they expand onto arable land), and are more energy efficient (Glaeser, 2012; Jenks, & Burgess, 2000; Yeang, 1999). According to the building arrangement scenarios in this study, the volume of high-rise buildings is 1.6 times higher than low-rise buildings on the same footprint, whereas the land area available for greenspace was 1.34 times higher under the high-rise scenario. Assuming that the housed population is 1.6 times higher in high-rise buildings than low-rise buildings, and then per capita land availability for public greenspace would be slightly less for people inhabiting high-rise buildings. However, the high-rise development we examined had fragments surrounding land to a lesser degree (due to there being fewer buildings), meaning that there would be more area available for public greenspaces (e.g., pocket parks) outside a high-rise's footprint.

5. Conclusion

This paper reports the results of the comparative and combinative effects of different spatial arrangements of two principal three-dimensional urban landscapes by integrating numerical and *in situ* meteorological measurements. Three contributory factors were considered in the present study, including building arrangement, amount of land covered by tree canopies, and intensity of solar irradiation relative to latitude. Our results provide three interesting insights that relate to mitigation UHI effects:

1. Both building and tree arrangements obviously influence thermal microclimates. High-rise developments have comparative advantage in saving more land, which can be used for greenspace development.

2. Increasing forested greenspace seems to lead to lower outdoor temperatures near ground level, but the relationship between the cooling capacity and the vegetation coverage is not linear. That is, the first 5% incremental increase in forest coverage (0% to 5%) showed the strongest cooling effect, whereas subsequent 5% incremental increases in forest cover showed gradually fewer cooling effects. Therefore, an optimal greenspace could be predicted that provides the most efficient vegetation cooling effect. Determining the optimal greenspace area is essential for improving urban environment and population health.

3. During the midday period, intense solar irradiation suppresses the cooling effects of mitigation strategies, such as increasing a certain amount of greenspace in urban environments with both high-rise and low-rise building developments. When we apply the LCZ classification in the future to estimate the urban inner spatial heterogeneity of thermal environments, we should pay more attention to thermal conditions that occur after sunset when the impacts of buildings and greenspace on the thermal environment are more discernable.

This study provides some insights into how buildings and greenspace together influence thermal comfort outdoors, information that can be used by urban planners and designers to generate more evidence-based guidelines for improving outdoor thermal comfort levels when developing high-density residential areas.

Acknowledgements

This work was supported by the National Science Foundation of China (41801182, 41590841). We are grateful to the anonymous reviewers for their constructive suggestions. We also express our gratitude to Prof. Michael Bruse and his team for providing the ENVI-met software.

References

Andreou, E. (2014). The effect of urban layout, street geometry and orientation on shading conditions in urban canyons in the Mediterranean. *Renewable Energy,* 63, 587-596.

Berkovic, S., Yezioro, A., & Bitan, A. (2012). Study of thermal comfort in courtyards in a hot arid climate. *Solar Energy,* 86, 1173-1186.

Bowler, D. E., Buyung-Ali, L., Knight, T. M., & Pullin, A. S. (2010). Urban greening to cool towns and cities: A systematic review of the empirical evidence. *Landscape and Urban Planning,* 97, 147-155.

Carfan, A. C., Galvani, E., & Nery, J. T. (2012). Study of thermal comfort in the City of São Paulo using ENVI-met model. *Investigaciones Geográficas, Boletín del Instituto de Geografía,* 78, 34-47.

Chang, C.-R., & Li, M.-H. (2014). Effects of urban parks on the local urban thermal environment. *Urban Forestry & Urban Greening,* 13, 672-681.

Chow, W. T. L., Pope, R. L., Martin, C. A., & Brazel, A. J. (2011). Observing and modeling the nocturnal park cool island of an arid city: horizontal and vertical impacts. *Theoretical and Applied Climatology,* 103, 197-211.

Coseo, P., & Larsen, L. (2014). How factors of land use/land cover, building configuration, and adjacent heat sources and sinks explain Urban Heat Islands in Chicago. *Landscape and Urban Planning,* 125, 117-129.

Ghaffarianhoseini, A., Berardi, U., & Ghaffarianhoseini, A. (2015). Thermal performance characteristics of unshaded courtyards in hot and humid climates. *Building and Environment,* 87 154-168.

Giridharan, R., Emmanuel, R. (2018). The impact of urban compactness, comfort strategies and energy consumption on tropical urban heat island intensity: *A review. Sustainable Cities and Society*, 40, 677-687.

Glaeser, E. (2012). Triumph of the City: How Our Greatest Invention Makes Us Richer, Smarter, Greener, Healthier, and Happier. Penguin Books. London. pp. 352.

Hondula, D. M., Barnett, A. G. (2014). Heat-related morbidity in Brisbane, Australia: Spatial variation and area-level predictors. *Environmental Health Perspectives*, 122, 831-836.

Jenks, M., & Burgess, R. (2000). Compact cities-sustainable urban forms for developing countries. Spon Press. New York.

Jiao, M., Zhou, W., Zheng, Z., Wang, J., & Qian, Y. (2017). Patch size of trees affects its cooling effectiveness: A perspective from shading and transpiration processes. *Agricultural and Forest Meteorology*, 247, 293-299.

Johansson, L., Onomura, S., Lindberg, F., & Seaquist, J. (2015). Towards the modelling of pedestrian wind speed using high-resolution digital surface models and statistical methods. *Theoretical and Applied Climatology*, 1-15.

Le, Z., & Jinsheng, G. (2008). Review and expectation on design of residential tower in Beijing. *Urbanism and Architecture*, 1, 33-36(In Chinese).

Leconte, F., Bouyer, J., Claverie, R., & Petrissans, M. (2015). Using Local Climate Zone scheme for UHI assessment: Evaluation of the method using mobile measurements. *Building and Environment*, 83, 39-49.

Lehnert, M., Geletič, J., Husák, J., & Vysoudil, M. (2014). Urban field classification by "local climate zones" in a medium-sized Central European city: the case of Olomouc (Czech Republic).

Theoretical and Applied Climatology, DOI 10.1007/s00704-014-1309-6,

Lehnert, M., Geletič, J., Husák, J., & Vysoudil, M. (2015). Urban field classification by "local climate zones" in a medium-sized Central European city: the case of Olomouc (Czech Republic). *Theoretical and Applied Climatology*, 122, 531-541.

Li, G., Zhou, M., Cai, Y., Zhang, Y., & Pan, X. (2011). Does temperature enhance acute mortality effects of ambient particle pollution in Tianjin City, China. *Science of The Total Environment*, 409, 1811-1817.

Li, X., Zhou, W., Ouyang, Z., Xu, W., & Zheng, H. (2012). Spatial pattern of greenspace affects land surface temperature: evidence from the heavily urbanized Beijing metropolitan area, China. *Landscape Ecology*, 27, 887-898.

Liu, Y., Theller, L. O., Pijanowski, B. C., & Engel, B. A. (2016). Optimal selection and placement of green infrastructure to reduce impacts of land use change and climate change on hydrology and water quality: An application to the Trail Creek Watershed, Indiana. *Science of The Total Environment*, 553, 149-163.

Middel, A., Chhetri, N., & Quay, R. (2014). Urban forestry and cool roofs: Assessment of heat mitigationstrategies in Phoenix residential neighborhoods. *Urban Forestry & Urban Greening*, 14 178-186.

Oke, T. R. (1987). The boundary layer climates. Methuen. London and New York, NY, USA.

Ratti, C., Raydan, D., & Steemers, K. (2003). Building form and environmental performance: archetypes, analysis and an arid climate. *Energy and Buildings*, 35, 49-59.

Shi, X., & Yang, J. (2014). A material flow-based approach for diagnosing urban ecosystem health. *Journal of Cleaner Production*, 64, 437-446.

Skelhorn, C., Lindley, S., & Levermore, G. (2014). The impact of vegetation types on air and surface temperatures in a temperate city: A fine scale assessment in Manchester, UK. *Landscape and Urban Planning,* 121, 129-140.

Sodoudi, S., Zhang, H., Chi, X., Müller, F., & Li, H. (2018). The influence of spatial configuration of green areas on microclimate and thermal comfort. *Urban Forestry & Urban Greening*, 34, 85-96.

Stewart, I. D. (2011). Redefining the Urban Heat Island, in: *Department of Geography*. Arizona State University. Vancouver. pp. 368.

Taleb, D., & Abu-Hijleh, B. (2013). Urban heat islands: Potential effect of organic and structured urban configurations on temperature variations in Dubai, UAE. *Renewable Energy,* 50, 747-762.

Taleghani, M., Tenpierik, M., van den Dobbelsteen, A., & de Dear, R. (2013). Energy use impact of and thermal comfort in different urban block types in the Netherlands. *Energy and Buildings*, 67, 166-175.

Tan, C. L., Wong, N. H., Tan, P. Y., Jusuf, S. K., & Chiam, Z. Q. (2015). Impact of plant evapotranspiration rate and shrub albedo on temperature reduction in the tropical outdoor environment. *Building and Environment,* 94, Part 1, 206-217.

Tian, G., & Qiao, Z. (2014). Assessing the impact of the urbanization process on net primary productivity in China in 1989-2000. *Environmental Pollution,* 184, 320-326.

Unger, J., Skarbit, N., & Gál, T. (2018). Evaluation of outdoor human thermal sensation of local climate zones based on long-term database. *International Journal of Biometeorology,* 62, 183-193.

Vaz Monteiro, M., Doick, K. J., Handley, P., & Peace, A. (2016). The impact of greenspace size on

the extent of local nocturnal air temperature cooling in London. *Urban Forestry & Urban Greening*, 16, 160-169.

Verdonck, M.-L., Demuzere, M., Hooyberghs, H., Beck, C., Cyrys, J., Schneider, A., et al. (2018). The potential of local climate zones maps as a heat stress assessment tool, supported by simulated air temperature data. *Landscape and Urban Planning*, 178, 183-197.

Wang, B., Koh, W. S., Liu, H., Yik, J., & Bui, V. P. (2017). Simulation and validation of solar heat gain in real urban environments. *Building and Environment*,123, 261-276.

Wang, J., & Ouyang, W. (2017). Attenuating the surface Urban Heat Island within the Local Thermal Zones through land surface modification. *Journal of Environmental Management*, 187, 239-252.

Ward, K., Lauf, S., Kleinschmit, B., & Endlicher, W. (2016). Heat waves and urban heat islands in Europe: A review of relevant drivers. *Science of The Total Environment*, 569–570, 527-539.

Wong, L., Alias, H., Aghamohammadi, N., Aghazadeh, S., & Nik Sulaiman, N. (2017). Urban heat island experience, control measures and health impact: A survey among working community in the city of Kuala Lumpur. *Sustainable Cities and Society*, 35, 660-668.

Xiao, X. D., Dong, L., Yan, H., Yang, N., & Xiong, Y. (2018). The influence of the spatial characteristics of urban green space on the urban heat island effect in Suzhou Industrial Park. *Sustainable Cities and Society*, 40, 428-439.

Xie, X., Huang, Z., & Wang, J.-s. (2005). Impact of building configuration on air quality in street canyon. *Atmospheric Environment*, 39, 4519-4530.

Xu, Y., Ren, C., Ma, P., Ho, J., Wang, W., Lau, K. K.-L., et al. (2017). Urban morphology detection and computation for urban climate research. *Landscape and Urban Planning*, 167, 212-224.

Yang, X., & Li, Y. (2015). The impact of building density and building height heterogeneity on average urban albedo and street surface temperature. *Building and Environment,* 90, 146-156.

Yeang, K. (1999). The green skyscraper : the basis for designing sustainable intensive buildings. Prestel. New York.

Yin, C., Yuan, M., Lu, Y., Huang, Y., & Liu, Y. (2018). Effects of urban form on the urban heat island effect based on spatial regression model. *Science of The Total Environment,* 634, 696-704.

Yu, C., & Hien, W. N. (2006). Thermal benefits of city parks. *Energy and Buildings*, 38, 105-120.

Yu, B., Liu, H., Wu, J., & Lin, W. (2009). Investigating impacts of urban morphology on spatio-temporal variations of solar radiation with airborne LIDAR data and a solar flux model: A case study of downtown Houston. *International Journal of Remote Sensing*, 30(17), 4359-4385.

Zeng, W., Lao, X., Rutherford, S., Xu, Y., Xu, X., Lin, H., et al. (2014). The effect of heat waves on mortality and effect modifiers in four communities of Guangdong Province, China. *Science of The Total Environment,* 482-483, 214-221.